European Polymer Journal 72 (2015) 620–631

Contents lists available at ScienceDirect

European Polymer Journal

journal homepage: www.elsevier.com/locate/europolj

Alginate microgels loaded with temperature sensitive liposomes for magnetic resonance imageable drug release and microgel visualization

Merel van Elk [a], Cyril Lorenzato [b], Burcin Ozbakir [a], Chris Oerlemans [b,c], Gert Storm [a], Frank Nijsen [c], Roel Deckers [b], Tina Vermonden [a], Wim E. Hennink [a,*]

[a] Department of Pharmaceutics, Utrecht Institute for Pharmaceutical Sciences, Utrecht University, Utrecht, The Netherlands
[b] Image Sciences Institute, University Medical Center Utrecht, Utrecht, The Netherlands
[c] Department of Radiology and Nuclear Medicine, University Medical Center Utrecht, Utrecht, The Netherlands

ARTICLE INFO

Article history:
Received 18 December 2014
Received in revised form 27 February 2015
Accepted 8 March 2015
Available online 12 March 2015

Keywords:
Temperature responsive liposomes
Alginate microspheres
Triggered release
Magnetic resonance imaging
Holmium ions
MRI contrast agent

ABSTRACT

The objective of this study was to prepare and characterize alginate microgels loaded with temperature sensitive liposomes, which release their payload after mild hyperthermia. It is further aimed that by using these microgels both the drug release and the microgel deposition can be visualized by magnetic resonance imaging (MRI) after their administration (e.g. in the vicinity of a tumor). To this end, temperature sensitive (TSL) and non-temperature sensitive liposomes (NTSL) loaded with fluorescein (drug mimicking dye) and a T_1 MRI contrast agent (Prohance®, [Gd(HPDO3A)(H_2O)]) were encapsulated in alginate microgels crosslinked by holmium ions (T_2^* MRI contrast agent). The drug release could be monitored by the release of [Gd(HPDO3A)(H_2O)] while the microgels could be visualized using MRI via the holmium ions in the microgels. The microgels were prepared with a JetCutter and had an average size of 325 μm and contained ~0.6 wt% Ho^{3+}.

Microgels loaded with NTSL (NTSL-Ho-microgels) were stable at 37 and 42 °C with only a minimal release of fluorescein and [Gd(HPDO3A)(H_2O)]. Microgels encapsulating TSL (TSL-Ho-microgels) released fluorescein and [Gd(HPDO3A)(H_2O)] only marginally at 37 °C while, importantly, their payload was co-released within 2 min at 42 °C. TSL-Ho-microgels were administered in an *ex vivo* sheep kidney via a catheter. Clusters of TSL-Ho-microgels could be visualized via MRI and were deposited in the interlobular blood vessels. In conclusion, these alginate TSL-Ho-microgels are promising systems for real-time, MR-guided embolization and triggered release of drugs *in vivo*.

Abbreviations: MRI, magnetic resonance imaging; NTSL, non-temperature sensitive liposomes; TSL, temperature sensitive liposomes; Gd, gadolinium; [Gd(HPDO3A)(H_2O)], Gd complex used as MRI contrast agent (Prohance®); Ho, holmium; Ba, barium; NTSL-Ho-microgels, holmium crosslinked microgels encapsulating NTSL; TSL-Ho-microgels, holmium crosslinked microgels encapsulating TSL; TACE, transarterial chemoembolization; DEB, drug eluting bead; DSPC, 1,2-distearoyl-*sn*-glycero-3-phosphocholine; DSPE-PEG2000, 1,2-distearoyl-*sn*-glycero-3-phosphoethanolamine-*N*-[amino(polyethylene glycol)-2000]; MSPC, 1-stearoyl-2-hydroxy-*sn*-glycero-3-phosphocholine; DPPC, 1,2-dipalmitoyl-*sn*-glycero-3-phosphocholine.

* Corresponding author at: Department of Pharmaceutics, Utrecht Institute for Pharmaceutical Sciences, Utrecht University, 3584 CG Utrecht, The Netherlands. Tel.: +31 0302517839.
E-mail address: W.E.Hennink@uu.nl (W.E. Hennink).

http://dx.doi.org/10.1016/j.eurpolymj.2015.03.013
0014-3057/

1. Introduction

The success of systemic administration of chemotherapeutic drugs is limited by the unfavorable balance of therapeutic drug concentrations in the tumor and toxic concentrations in healthy tissues. Nanosized drug delivery systems have been developed to improve the therapeutic efficacy and/or to reduce unwanted side effects of chemotherapeutic drugs. These delivery systems can accumulate in the tumor after intravenous injection via the enhanced permeability and retention (EPR) effect [1–5]. Liposomes are the most intensively studied drug delivery systems so far [6–10] and a number of studies showed that encapsulation of doxorubicin (DOX) in liposomes resulted in an increased therapeutic index, particularly due to significantly reduced cardio toxicity and other unwanted side effects. Liposomal DOX showed a significant improvement in response rate from 25% to 46% compared to standard combination chemotherapy for the treatment of kaposi's carcinoma [11]. On the contrary, the anti-tumor efficacy in patients with metastatic breast cancer was not improved by liposomal DOX [12,13]. This variation in anti-tumor efficacy between tumor types can be explained by the heterogeneous nature of the EPR effect since this phenomenon varies between tumor models, from patient to patient and even varies within one tumor [2,14]. Triggerable liposomal drug release systems can locally release their therapeutic payload in the tumor. Temperature sensitive liposomes have been shown to release their drug content fast at elevated temperatures [15–18] and induce higher peak concentrations at the tumor site after local heat treatment compared to administration of free drug or conventional drug containing liposomes [19–21].

Localized drug delivery of chemotherapeutics can also be achieved via transarterial chemoembolization (TACE). During the TACE procedure, a catheter is positioned in the arterial supply of a tumor via which a chemotherapeutic drug is administered followed by embolic particles [22,23]. These embolic particles occlude the blood vessels preferably in the tumor, leading to a restricted or even loss of blood flow, resulting in ischemia of the tumor. The blockage of the blood vessels by the embolic particles also reduces the washout of the chemotherapeutic drug and therefore minimizes systemic exposure [23,24].

Recently, drug eluting beads (DEB), which consist of embolic particles loaded with a chemotherapeutic drug, have been developed to simplify and standardize the TACE procedure since chemotherapeutic drugs and the embolic particles are delivered simultaneously [23,25,26]. Examples of polymers used for the preparation of DEBs are chitosan [27,28], PLGA (poly(lactide-co-glycolide)) [29] and alginate [30]. Clinically used DEBs are based on polyvinyl alcohol modified with a sulfonic acid group to obtain negatively charged microspheres (DC beads). A high loading of positively charged cytostatics such as doxorubicin and irinotecan can be achieved in these PVA DEBs via an ion exchange mechanism [26,31,32]. Clinical trials have shown that embolization with DEB leads to a significant reduction in peak plasma concentration and area under the curve of doxorubicin [33,34] while increasing the antitumor efficacy compared to conventional TACE [35,36].

A drawback of these clinically used DEBs is however that they lack the ability to be visualized during and after administration. Therefore, it is not possible to monitor whether microspheres are deposited in the tumor or that they are located outside tumor tissue. Also the drug distribution cannot be monitored *in vivo*, making it difficult to predict the efficacy in the tumor. The beads which are currently used for chemoembolization have a sustained release profile. As a result, the drug is slowly released leading to relatively low tumor concentration. With our formulation we aim for triggered drug release, resulting in local high concentration of the antitumor agent. To support this assumption, it was previously shown that high concentrations of DOX in the tumor resulted in a high cellular uptake of this drug [37]. Further, in another study a good correlation was found between the intracellular DOX concentration and the antitumor efficacy [38].

To overcome these challenges, this research aims to prepare microgels that can be visualized in all stadia of treatment. The administration and microgel distribution can be visualized because the used polymer, alginate, is crosslinked with a T_2^* MRI contrast agent (holmium ions) which can be visualized by magnetic resonance imaging (MRI) [39]. The triggered drug release from these alginate microgels by encapsulating temperature sensitive liposomes can be visualized by a T_1 MRI contrast agent ([Gd(HPDO3A)-(H_2O)]) which is loaded in the liposomes. In principle, besides monitoring the drug release also the tumor penetration can be visualized (Fig. 1). For clinical application of TACE, the diameter of the microgels should be around 300 μm [40].

Alginate was selected for the preparation of microgels since crosslinked microgels can be prepared via a simple procedure [41–43]. The monodisperse alginate microgels can be prepared easily by JetCutting [44,45]. Importantly, mild crosslinking conditions are used, allowing encapsulation of liposomes in alginate microgels [46–48]. Thereby, crosslinking with Ho^{3+} (T_2^* MRI contrast agent) is possible and allows MRI visualization [49]. Finally, alginate microgels have previously been used for arterial embolization. No reopening of the arteries was observed on an angiogram up to 8 weeks after embolization, indicating that alginate microgels are suitable materials for embolization [30,50,51].

2. Materials and methods

2.1. Materials

1,2-Dipalmitoyl-*sn*-glycero-3-phosphocholine (DPPC), 1,2-distearoyl-*sn*-glycero-3-phosphocholine (DSPC) and 1,2-distearoyl-*sn*-glycero-3-phosphoethanolamine-*N*-[amino-(polyethylene glycol)-2000] (DSPE-PEG2000) were purchased from Lipoid GmbH, Ludwigshafen, Germany. 1-Stearoyl-2-hydroxy-*sn*-glycero-3-phosphocholine (MSPC) was obtained from Avanti Polar Lipids, Alabaster, U.S.A.

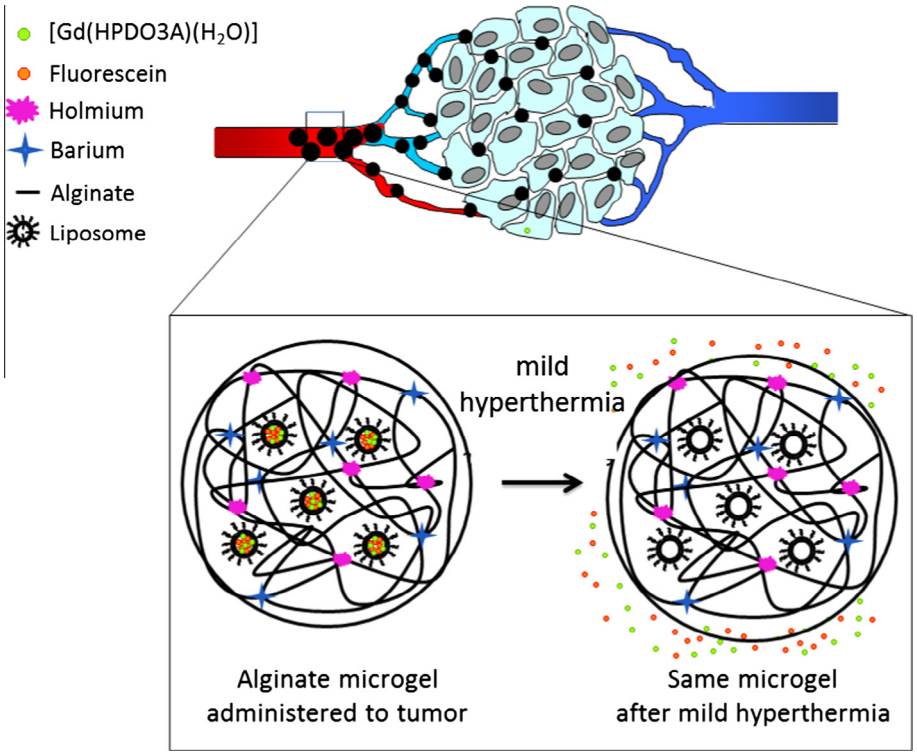

Fig. 1. Schematic representation of accumulation of alginate microgels with encapsulated temperature sensitive liposomes in a tumor during embolization. The alginate microgels are crosslinked with holmium ions to allow microgel visualization by magnetic resonance imaging (MRI). Upon mild hyperthermia, the liposomes will release their payload (fluorescein (drug mimicking dye) and [Gd(HPDO3A)(H_2O)] (MRI agent)). This release of [Gd(HPDO3A)(H_2O)] can also be monitored with MRI.

Cholesterol and barium chloride dehydrate were purchased from Sigma–Aldrich Chemie BV, Zwijndrecht, The Netherlands. Holmium chloride hexahydrate was obtained from Metall rare earth limited, Shenzhen, China. Fluorescein disodium for injection was obtained from Fresenius Kabi Nederland BV, s-Hertogenbosch, The Netherlands. [Gd(HPDO3A)(H_2O)] (Prohance®) was purchased from Bracco Diagnostic Inc., Monroe Township, U.S.A. Sodium alginate (Manucol LKX) was a gift from FMC biopolymer, Philadelphia, U.S.A.

2.2. Preparation of empty alginate microgels crosslinked with varying holmium- and barium-ion content

Holmium crosslinked alginate microgels (Ho-microgels) were prepared with a JetCutter (GeniaLab® BioTechnology, Germany) [44,49]. In detail, sodium alginate (3% w/v) was dissolved overnight under magnetic stirring in 20 mM HEPES buffer pH 7.4 also containing 8 g NaCl/L. Air bubbles were removed by sonication. The JetCutter was equipped with a nozzle with a diameter of 150 μm and a cutting tool having 120 wires with a thickness of 100 μm. The rotor speed was 5000 rpm and the alginate flow was set at 0.3 g/s. The alginate droplets were collected in 1 L of 20 mM HEPES buffer pH 7.4 containing different ratios of holmium chloride and barium chloride (0:100–100:0) with a total cation concentration of 100 mM. The formed microgels were hardened for 2 h and subsequently washed three times with 20 mM HEPES buffer pH 7.4 (in total 0.5–1 L) to remove the excess of crosslinking ions.

2.3. Preparation of liposomes

Two different liposomal formulations were prepared: non-temperature sensitive liposomes (NTSL) composed of DSPC, cholesterol and DSPE-PEG2000 (in molar ratio of 56:39:5) and temperature sensitive liposomes (TSL) composed of DPPC, MSPC and DSPE-PEG2000 (molar ratio of 86:10:4) [52,53]. A lipid film was formed by dissolving the lipids and cholesterol in 10 mL chloroform (160 μmol total lipids/mL) followed by rotary evaporation of the solvent under reduced pressure in a 100 mL round bottom flask. The resulting lipid film was further dried overnight under a nitrogen flow. The lipid film was hydrated in water for injection (20 mL) containing 0.375 mM [Gd(HPDO3A)(H_2O)] and 25 mg/mL fluorescein at 60 °C. The liposomal dispersion (80 μmol total lipid/mL) was extruded through two 200 nm filters (2 times) and two 100 nm filters (8 times). Liposomes were passed three times through a PD-10 column to remove unencapsulated fluorescein and [Gd(HPDO3A)(H_2O)].

2.4. Preparation of alginate microgels loaded with liposomes (NTSL/TSL-Ho-microgels)

NTSL/TSL-Ho-microgels were prepared by mixing a sodium alginate solution (4% w/v in 20 mM HEPES buffer

pH 7.4) with NTSL or TSL (80 μmol total lipid/mL) in a 3:1 ratio. The alginate solution was processed by the JetCutter with the same settings as described above. The alginate droplets containing NTSL or TSL were crosslinked with a holmium:barium molar ion ratio of 5:95 to form NTSL/TSL-Ho-microgels. The total cation concentration during crosslinking was 100 mM.

2.5. Light microscopy

Morphological examination and size distribution of NTSL/TSL-Ho-microgels were investigated with light microscopy. Microgels were suspended in 20 mM HEPES buffer pH 7.4 (100 mg microgels/mL) and subsequently some droplets were pipetted on a microscopy slide. The size of the microgels was examined using light microscopy with phase contrast (Eclipse E200, Nikon equipped with a DS-Fi1 camera, Nikon and a E plan 10× lens, Nikon). The images were analyzed with NIS-elements D 3.0 software to determine the microgel diameter. The average size of the microgels was calculated by averaging the diameter of 100 microgels.

2.6. Analysis of holmium content in microgels

The amount of holmium ions in the microgels was determined via complexometric analysis. Wet microgels (150 mg) were destructed in nitric acid (65%, ±15 mL) at 100 °C till the solution became transparent (±30 min). Hexamine (5 g) was added and the pH of the solution was adjusted with 10 M sodium hydroxide to 5.0–5.5. Next, xylenol-orange (50 mg, 1:100 mixture in potassium nitrate) was added and the solution was titrated with 10 mM ethylenediaminetetraacetic acid (EDTA) till a color shift to yellow was visually observed [45]. The weight percentage of holmium ions present in the microgels was calculated with the following equation: (titer EDTA × mL EDTA) × (molecular weight of Ho (164.93 g/mol))/mg microgels. The concentration of holmium ions and monomer units in the microgels was calculated to determine the ratio between holmium ions and alginate monomer units. The microgels contain 3 wt% alginate.

2.7. Dynamic light scattering

The size of the liposomes and the polydispersity index were measured with dynamic light scattering at 25 °C (DLS; Malvern CGS-3 multiangle goniometer). Intensity correlation functions were measured using a wavelength of 632.8 nm and a scattering angle of 90°. The measurements were performed in 20 mM HEPES buffer pH 7.4.

2.8. Determination of fluorescein concentration

The fluorescein concentration in the liposomes was determined after disruption of the liposomes by addition of a small volume of 10% Triton-X100 in water to the liposomal dispersion (final concentration of Tritox-X100 was 0.1%) using fluorescence measurements (excitation wavelength 500 nm, emission wavelength 520 nm). The encapsulation efficiency of NTSL and TSL in NTSL-Ho-microgels as well as in TSL-Ho-microgels was determined by measuring the fluorescein concentration in the microgels by disrupting the liposomes in the microgels with Triton-X100.

2.9. MR imaging

Magnetic resonance imaging (MRI) was used to visualize the holmium crosslinked microgels and to monitor the temperature triggered [Gd(HPDO3A)(H_2O)] release from the liposomes that were entrapped in the microgels. All MRI experiments were performed on a clinical 1.5-Tesla MR scanner (Achieva; Philips Health care). The following MR sequences were used in this study. T_2^*-weighted gradient echo scans were acquired to visualize holmium crosslinked microgels (TR = 570.6 ms, TE = 9.72 ms, FA = 25°, turbo-factor = 32, 32 slices, voxel size = 0.96 × 0.96 × 2.0 mm^3). T_1-weighted spin echo scans (TR = 1000 ms, TE = 8 ms, FA = 90°, turbo-factor = 15, 3 slices, voxel size = 0.94 × 0.94 × 2.0 mm^3) were acquired and R_1-mapping was performed in order to monitor [Gd(HPDO3A)(H_2O)] release. R_1-maps were obtained by sampling the signal recovery after inversion using a Look-Locker (LL) sequence (TR = 4 s, TE = 2.75 ms, FA = 6°, turbo-factor = 5, 1 slice, voxel size = 0.94 × 0.94 × 5 mm^3, 104 timepoints at 29 ms interval).

The images obtained from each LL measurement were automatically fitted with in-house developed Matlab software (7.12, The MathWorks Inc., Natick, MA, USA, 2000). The temporal evolution of the magnitude of the longitudinal magnetization (M) was fitted (Levenberg–Marquardt algorithm) for each pixel with the following equation:

$$M = \left|A - \left[(A + B) \cdot e^{-t \cdot R_1^*}\right]\right| \quad (1)$$

where R_1^* is the apparent longitudinal relaxation rate, t is the time after the inversion pulse and A and B are constants. The sample R_1 differs from R_1^* by an offset only dependent on flip angle (α) and delay between 2 consecutive excitation pulses (Δt):

$$R_1 = R_1^* + \log(\cos\alpha)/\Delta t \quad (2)$$

A square ROI (5 × 5 pixels) was manually selected inside the sample to analyze the R_1 before and after heating.

2.10. Fluorescein release

The release of fluorescein from the liposomes and NTSL/TSL-Ho-microgels was measured by the change in fluorescence intensity in time (excitation wavelength 500 nm, emission wavelength 520 nm). Twenty-five mL of preheated 20 mM HEPES buffer pH 7.4 (37 or 42 °C, heated in water bath) was added to the liposome suspension (50 μl liposomes with 80 μmol total lipids/ml). Samples (1 mL) were taken at different time points (0, 2, 5, 10, 15, 30, 45 and 60 min) and subsequently cooled on ice to prevent further leakage. Triton X-100 (10%, 170 μL) was added at the end of the experiment to destroy remaining liposomes and release entrapped fluorescein. The percentage fluorescein released was calculated using the following

equation: $(I_t - I_0)/(I_{TX} - I_0) \times 100$ in which I_t is the fluorescence intensity at time t, I_0 the intensity at the start of the experiment and I_{TX} the fluorescence intensity after addition of Triton-X100.

The release of fluorescein from NTSL/TSL-Ho-microgels was measured at the same wavelengths as described for the liposomes. Fifty mL of preheated buffer was added to the microgels (1.5 g wet microgels). Microgels were shaken after which the microgels settled at the bottom due to gravity. Samples (1 mL) were taken at different time points (0, 2, 5, 10, 15, 30, 45 and 60 min) and subsequently cooled on ice to prevent further leakage. Triton X-100 (10%, 430 μL) was added to the microgel pellet to disrupt the intact liposomes loaded into the microgels. The percent fluorescein released was calculated as described above.

2.11. Fluorescence microscopy

Samples were prepared similarly as for the light microscopy measurements. The release of fluorescein from NTSL/TSL-Ho-microgels was visualized with a fluorescence microscope (BZ-9000, Keyence). A GFP BP filter with an excitation wavelength of 472–30 nm and emission wavelength of 520–35 nm and a Plan Fluor 20× lens (Nikon) was used. The images were analyzed with BZ II Analyzer software. NTSL/TSL-Ho-microgels were imaged in 20 mM HEPES buffer pH 7.4 at room temperature and after incubation at mild hyperthermia for 10 s.

2.12. Ex vivo embolization of a sheep kidney

The *ex-vivo* sheep kidney used as an *ex vivo* model for embolization was derived from a terminated female sheep that was previously used as laboratory animal. A catheter (Abocath 18G, Hospira, U.K.) was inserted into the renal artery and fixed with a suture. The kidney was placed in a plastic bucket fillet with H_2O containing 0.8% NaCl at room temperature. TSL-Ho-microgels crosslinked with 5 mM holmium ions (75 mg wet weight in 1 mL 20 mM HEPES buffer pH 7.4) were administered via the catheter. A T_2^*-weighted MRI scan was made before and after injection of the microgels.

2.13. Statistical analysis

Statistical analysis was performed with the software GraphPad Prism 6.01. A 2-way ANOVA was performed followed by a Tukey test for statistical analysis at different temperatures or a Sidak test for statistical analysis of the different microgel formulations.

3. Results and discussion

3.1. Characterization of empty alginate microgels

Alginate microgels were prepared by crosslinking alginate dissolved in 20 mM HEPES buffer pH 7.4 with di (Ba^{2+}) or trivalent ions (Ho^{3+}) using a JetCutter. Holmium containing particles are paramagnetic contrast agents inducing local magnetic field variations that cause dephasing of the MR signal, which results in local signal voids. Barium based particles do not exhibit these paramagnetic characteristics. Fig. 2 shows T_2^*-weighted (wt) and T_1-wt images of microgels that were prepared by crosslinking alginate with different ratios of holmium and barium ions. The microgels contained 0–1.35% of holmium (w/wet weight microgels), which correlates with a holmium ion to alginate monomer ratio of 0–0.54 (Table 1). The monomer concentration was calculated assuming that the microgels contain 3% alginate. Microgels crosslinked with solely holmium ions had a holmium ion to alginate monomer ratio of 0.54:1 indicating that one holmium ion

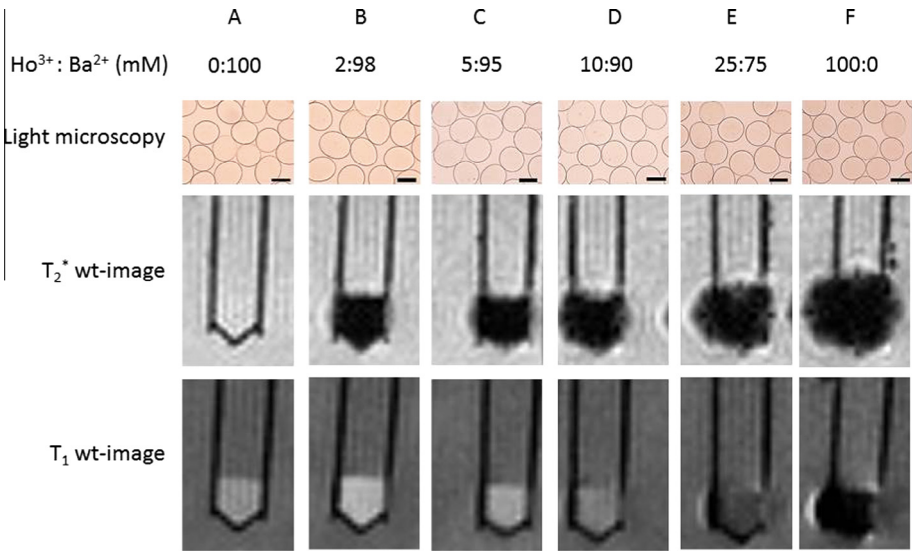

Fig. 2. Top: Light microscopy images of alginate microgels crosslinked using different holmium and barium ion concentrations. The scale bar represents 200 μm. (mM Ho:Ba in crosslinking solution, A 0:100, B 2:98, C: 5:95, D 10:90, E 25:75 and F 100:0). Middle: T_2^* wt-image of sedimented alginate microgels crosslinked using different holmium and barium ion concentrations. Bottom: T_1 wt-image of sedimented alginate microgels crosslinked using different holmium and barium ion concentrations.

Table 1
Characteristics of alginate microgels crosslinked with different holmium:barium ratios with a total cation concentration of 100 mM. Microgels were prepared using a JetCutter.

mM Ho	Ho content (% w/w, wet weight)[a]	Ho:monomer unit (ratio mol/mol)	Mean size (μm)[b]
0	0	0	281 ± 21
2	0.24 ± 0.01	0.10:1	293 ± 20
5	0.30 ± 0.01	0.12:1	294 ± 19
10	0.47 ± 0.01	0.16:1	293 ± 20
25	0.72 ± 0.02	0.29:1	287 ± 19
100	1.35 ± 0.05	0.54:1	278 ± 15

[a] Determined by complexometric titration (standard deviation (sd) of 3 different measurements).
[b] Determined by light microscopy (sd refers to variation in size of microgels with $n = 100$).

crosslinks two monomer units which is in line with previous observations [45]. The diameter of the microgels ranged between 278 and 294 μm which is a clinically relevant size for transarterial chemoembolization of hepatocellular carcinoma [40]. The microgels had a narrow size distribution with a standard deviation of ~20 μm (Table 1 and Fig. 2). As expected, the microgels crosslinked only with barium ions were not detectable on T_2^*-wt images, whereas microgels crosslinked with increasing amounts of holmium ions showed increasing signal voids on these images. In contrast, on T_1-weighted spin echo images barium as well as holmium ion crosslinked microgels were detectable. Yet, with increasing holmium ion concentrations, the detected MR-signal in these T_1-weighted images decreased due to the pronounced T_2^*-effect. In subsequent experiments, we continued to work with microgels crosslinked with a holmium:barium ratio of 5:95. These microgels were detectable on T_2^*-wt gradient echo images and gave sufficient signal on T_1-wt spin echo images to detect [Gd(HPDO3A)(H_2O)] induced T_1 changes.

3.2. Characterization of temperature-sensitive and non-temperature sensitive liposomes encapsulating fluorescein and [Gd(HPDO3A)(H_2O)]

Temperature sensitive liposomes (TSL) containing lysolipids were prepared for encapsulation in alginate microgels. The incorporation of a lysolipid in the bilayer of liposomes enhances the release at mild hyperthermia [15,19,54]. It has been further shown that temperature sensitive liposomes containing 5% mol DSPE-PEG2000 were stable at 37 °C and showed complete content release at 42 °C [55]. Non-temperature sensitive liposomes (NTSL) were prepared as control.

Liposomes loaded with fluorescein and [Gd(HPDO3A)(H_2O)] (MRI-contrast agent) were prepared via the lipid film hydration method (Table 2). The mean size of NTSL and TSL were 108 and 133 nm, respectively, with a PDI ⩽ 0.1. The encapsulation efficiency of fluorescein was about 8% for the NTSL and 11% for the TSL. Such encapsulation efficiencies are expected since fluorescein dissolved in water is passively loaded into liposomes [56]. Likely, the extrusion loss is different for these formulations resulting in a slight difference in encapsulation efficiency.

Table 2
Characteristics of non-temperature sensitive (NTSL) and temperature sensitive liposomes (TSL) encapsulating fluorescein and [Gd(HPDO3A)(H_2O)].

	NTSL	TSL
Lipid composition	DSPC:Chol:DSPE-PEG2000	DPPC:MSPC:DSPE-PEG2000
Molar ratio lipids (feed ratio)	56:39:5	86:10:4
Mean size (nm)	108 ± 1 nm	133 ± 1 nm
PDI	0.07 ± 0.02	0.09 ± 0.02
Fluorescein encapsulation (%)	7.6	11.2

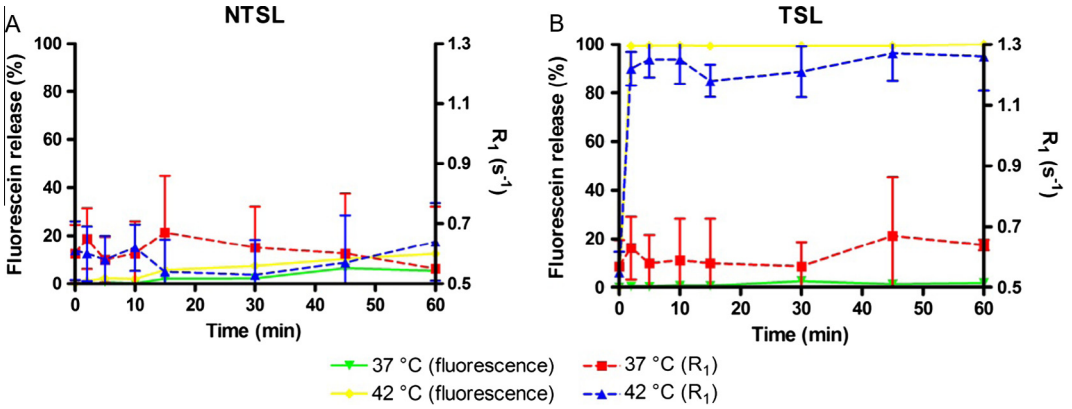

Fig. 3. Fluorescence signal and T_1 relaxation rate measured by MRI as function of incubation time at 37 and 42 °C for NTSL (A) and TSL (B). Liposomes were diluted in 20 mM HEPES buffer pH 7.4 to a total lipid concentration of 0.16 μmol/mL.

Table 3
Characteristics of NTSL-Ho-microgels and TSL-Ho-microgels prepared using a JetCutter.

	NTSL-Ho-microgels	TSL-Ho-microgels
Mean size (μm)	325 ± 17	323 ± 18
Ho content (% w/w, wet weight)	0.65 ± 0.03	0.59 ± 0.04
Ho:monomer unit (ratio mol/mol)	0.26:1	0.24:1
Liposome encapsulation (%)	91	97

Fig. 3 shows the fluorescence signal and T_1 relaxation rate (R_1) measured by MRI as function of incubation time at 37 and 42 °C for NTSL (A) and TSL (B). Hardly any release of fluorescein as well as [Gd(HPDO3A)(H_2O)] from the NTSL formulation was observed at 37 and 42 °C during 60 min, indicating that the NTSL formulation is stable at both 37 and 42 °C. The TSL formulation showed a slow release at 37 °C but released both fluorescein and [Gd(HPDO3A)(H_2O)] completely at the same rate within 2 min at 42 °C.

3.3. Preparation of holmium crosslinked alginate microgels containing NTSL or TSL (NTSL-Ho-microgels or TSL-Ho-microgels)

Alginate droplets containing NTSL or TSL were crosslinked by dropping them in a solution of 5 mM Ho^{3+} and 95 mM Ba^{2+} to form microgels (NTSL/TSL-Ho-microgels). Their characteristics are displayed in Table 3.

Both types of microgels had a mean size around 325 μm and displayed a very low size distribution (Table 3 and Fig. 4). There was no substantial difference between the diameter of empty alginate microgels (Table 1) and microgels loaded with liposomes (Table 3). Obviously the encapsulation of liposomes did not interfere adversely with the formation of alginate microgels [46,48]. These microgels crosslinked with 5 mM Ho^{3+} and 95 mM Ba^{2+} contained 0.6% holmium^{3+} (w/w, wet weight) corresponding to a holmium^{3+} to alginate monomer ratio of ~0.25 (mol/mol). Crosslinking alginate microgels with 100 mM holmium ions resulted in a holmium^{3+} to alginate monomer ratio of ~0.54 (Table 1). The relatively high Ho^{3+} ratio of gels prepared at a Ho^{3+}:Ba^{2+} feed ratio of 5:95 suggests that holmium^{3+} has a higher affinity for alginate chains than barium^{2+}. Alginate is a copolymer consisting of β-D-mannuronic acid (M) and α-L-guluronic acid (G) residues. Crosslinking occurs by di or trivalent ions that form bridges between dimers of MM, GG and GM. It has been reported that divalent ions preferably bind to GG dimers while trivalent ions bind to GG as well as to MM dimers [57]. Consequently, trivalent ions like holmium are incorporated into alginate gels to a larger extent than divalent ions such

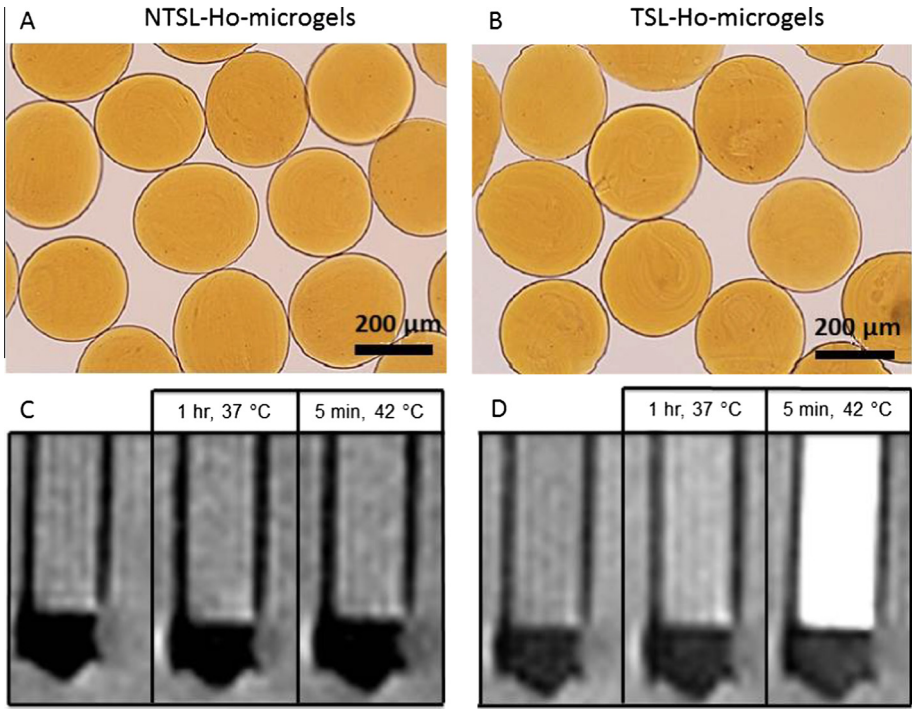

Fig. 4. Top: Light microscopy image of NTSL-Ho-microgels (A) and TSL-Ho-microgels (B) at room temperature. A black rim is observed around the microgels due to the difference in refractive index of the microgels and the surrounding medium [61].Bottom: T_1-wt MR images of NTSL-Ho-microgel (C) and TSL-Ho-microgel (D) dispersions at room temperature, after incubation at 37 °C (1 h) and 42 °C (5 min). Signal enhancement/whitening in the supernatant of the TSL-Ho-microgels at 42 °C indicates the release of [Gd(HPDO3A)(H_2O)].

as barium (Table 1). In a phase 1 clinical trial, the safety of holmium-166 microspheres is assed in patients with liver metastases. This clinical trial showed that embolization with holmium microspheres is a safe treatment option and the toxicity observed after administration of 600 mg microspheres was mainly associated with post embolization syndrome [58]. Thereby, the intraperitoneal LD_{50} of holmium salts in mice is 320–560 mg/kg [59,60]. NTSL/TSL-Ho-microgels crosslinked with 5 mM Ho^{3+} and 95 mM Ba^{2+} contain a relatively low concentration of holmium ions (⩽1% w/w), corresponding with ⩽6 mg holmium ions per 600 mg microgels. Therefore the toxicity of the microgels is expected to be low. Liposomes were encapsulated nearly quantitatively into the alginate microgels. The presence of fluorescein encapsulated in the liposomes loaded in the microgels could be observed with light microscopy; the NTSL/TSL-Ho-microgels are yellow due to the presence of fluorescein loaded liposomes while empty microgels are transparent (Figs. 2 and 4A–B). A modest variation in size and holmium content was observed between the empty and liposome loaded microgels (Table 1 and 3). The differences observed are batch-to-batch variations and are likely due to small variations in the processing variables (e.g. nitrogen pressure and flow rate are all manually set).

3.4. Release of fluorescein and [Gd(HPDO3A)(H_2O)] from NTSL-Ho-microgels and TSL-Ho-microgels

The release of [Gd(HPDO3A)(H_2O)] from the alginate microgels was visualized by T_1-wt MR images (Fig. 4C–D). During incubation for 1 h at 37 °C, both NTSL-Ho-microgels and TSL-Ho-microgels sedimented. A slight increase in signal intensity in the supernatant of the TSL-Ho-microgels was observed after incubation at 37 °C while no change in signal intensity was observed when NTSL-Ho-microgels were incubation at 37 °C. This indicates that [Gd(HPDO3A)(H_2O)] was not released from the NTSL-Ho-microgels (supernatant remained gray) and only marginally from the TSL-Ho-microgels after incubation at 37 °C for 1 h (∼5%). However, a significant signal enhancement was observed after mild hyperthermia (42 °C for 5 min) in the aqueous medium above the TSL-Ho-microgels (supernatant became white). This increase in signal demonstrates the release of [Gd(HPDO3A)(H_2O)] from TSL-Ho-microgels while under the same conditions no release of [Gd(HPDO3A)(H_2O)] from NTSL-Ho-microgels was detected.

Fig. 5 shows the signal intensity in the supernatant as well as in the microgel pellet for NTSL-Ho-microgels and TSL-Ho-microgels before mild hyperthermia, after incubation at 37 °C (1 h) and 42 °C (5 min). In correspondence with Fig. 4 no signal enhancement was detected neither in the microgel pellet nor in the supernatant for the NTSL-Ho-microgels at 37 and 42 °C. In contrast, there was a significant signal enhancement observed in the supernatant as well as in the microgel pellet upon incubation of the TSL-Ho-microgels at 42 °C, which indicates the release of [Gd(HPDO3A)(H_2O)]. When the signal intensities between the NTSL-Ho-microgels and the TSL-Ho-microgels are compared, a significantly higher signal is observed in the supernatant and microgel pellet of the TSL-Ho-microgels after incubation at 42 °C. This indicates that the TSL-Ho-microgels released at 42 °C. No significant difference in signal intensity was detected after incubation at 37 °C for 1 h. Therefore, NTSL-Ho-microgels as well as TSl-Ho-microgels did not release at this temperature.

Additionally, the release of fluorescein was examined (Fig. 6). Individual NTSL-Ho-microgels and TSL-Ho-microgels were imaged with a fluorescence microscope at room temperature and after mild hyperthermia for 10 s. Both types of microgels exhibited a homogeneous distribution of the fluorescein containing liposomes. For both NTSL-Ho-microgels and TSL-Ho-microgels no fluorescence signal was detected outside the microgels at room temperature indicating that all fluorescein remained encapsulated in the liposomes of NTSL/TSL-Ho-microgels. After mild hyperthermia, the fluorescence signal remained restricted to the NTSL-Ho-microgels. This indicates that the NTSL-Ho-microgels are stable during mild hyperthermia with no release of fluorescein. In contrast, after applying mild hyperthermia to TSL-Ho-microgels, the fluorescence signal was not restricted to the microgels only but also detected in the surrounding medium. This observation

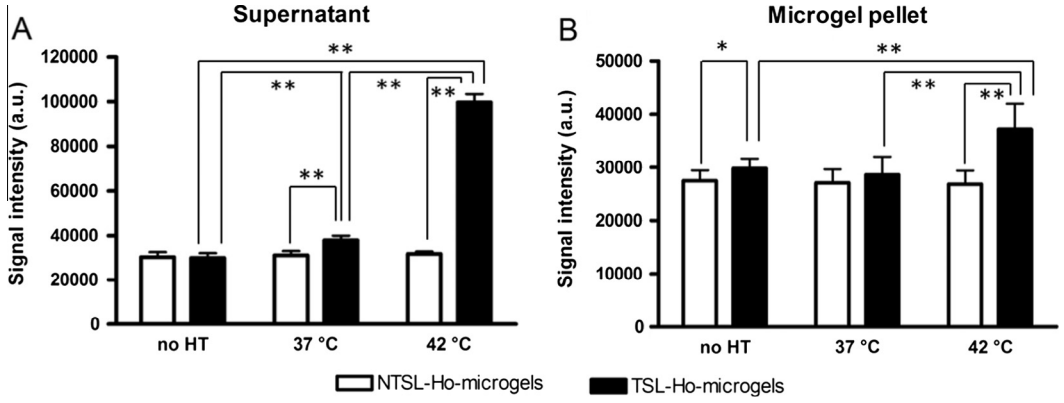

Fig. 5. Signal intensity in the supernatant (A) and microgel pellet (B) of NTSL-Ho-microgel and TSL-Ho-microgel dispersions at room temperature (RT) and after incubation at 37 °C (1 h) and 42 °C (5 min). An increase in signal intensity indicates the release of [Gd(HPDO3A)(H_2O)]. $^{*}p$ 0.01–0.05, $^{**}p < 0.0001$.

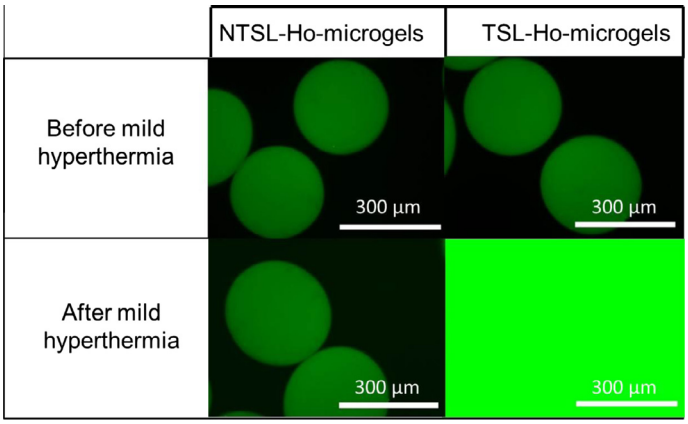

Fig. 6. Fluorescence microscopy images of NTSL/TSL-Ho-microgels at room temperature and after incubation at mild hyperthermia for 10 s. Fluorescein appears green in these fluorescence images. (For interpretation of the references to colour in this figure legend, the reader is referred to the web version of this article.)

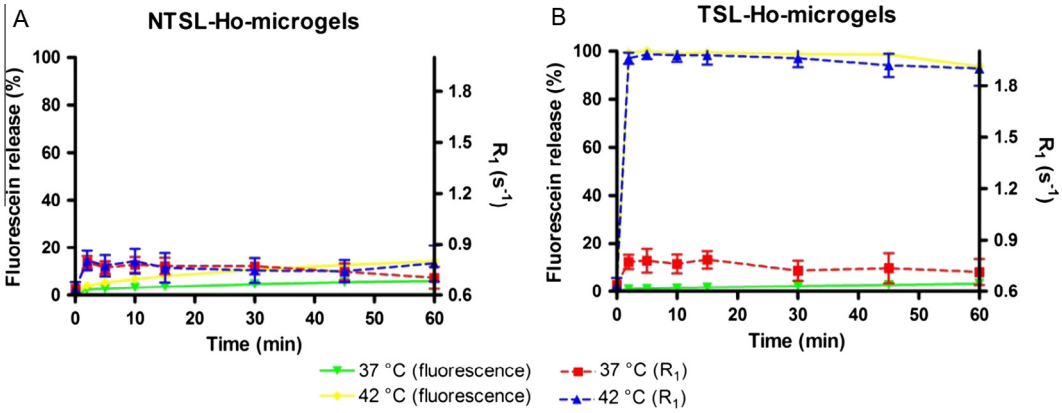

Fig. 7. Release of fluorescein and [Gd(HPDO3A)(H_2O)] from NTSL-Ho-microgels (A) and TSL-Ho-microgels (B) at 37 and 42 °C in 20 mM HEPES buffer pH 7.4.

demonstrates that fluorescein was released from TSL-Ho-microgels.

To investigate whether fluorescein and [Gd(HPDO3A)(H_2O)] are released completely and with the same kinetics, the release was monitored at 37 and 42 °C for 60 min (Fig. 7). NTSL-Ho-microgels displayed hardly any release of fluorescein or [Gd(HPDO3A)(H_2O)] at 37 or 42 °C for 60 min, which is in line with the lack of release in case of NTSL only (Fig. 4). As can be seen in Fig. 7B, TSL-Ho-microgels released fluorescein and [Gd(HPDO3A)(H_2O)] only marginally at 37 °C demonstrating that TSL encapsulated in microgels do not release both markers at this temperature. When increasing the temperature to 42 °C, TSL-Ho-microgels released both fluorescein and [Gd(HPDO3A)(H_2O)] completely within 2 min. For both types of microgels (containing NTSL or TSL) the release kinetics matches the kinetics of the liposomes not encapsulated in microgels at the investigated temperatures.

This observation indicates that diffusion of fluorescein and [Gd(HPDO3A)(H_2O)] released after destabilization of the entrapped liposomes through the alginate matrix is fast. Alginate forms an open network after crosslinking and a mesh size between 10 and 60 nm has been reported after crosslinking a 2% alginate solution [62,63]. In this study, we used a higher alginate concentration (3% w/v), which increases the number of crosslinks resulting in a smaller mesh size. This mesh size is small enough to retain liposomes while small molecules like fluorescein (0.7 nm [64], 332.31 g/mol) and [Gd(HPDO3A)(H_2O)] (558.7 g/mol) can diffuse freely from this matrix. Furthermore, the fast release of fluorescein and [Gd(HPDO3A)(H_2O)] also demonstrates that no strong interactions between fluorescein/[Gd(HPDO3A)(H_2O)] and alginate exist.

3.5. Ex vivo embolization of a sheep kidney

The *ex-vivo* sheep kidney used as an *ex vivo* model for embolization was derived from a terminated female sheep that was previously used as laboratory animal. A T_2^*-wt MR image of the *ex vivo* kidney before and after administration of TSL-Ho-microgels is shown in Fig. 8. Prior to administration, the kidney tissue appeared relatively homogeneously

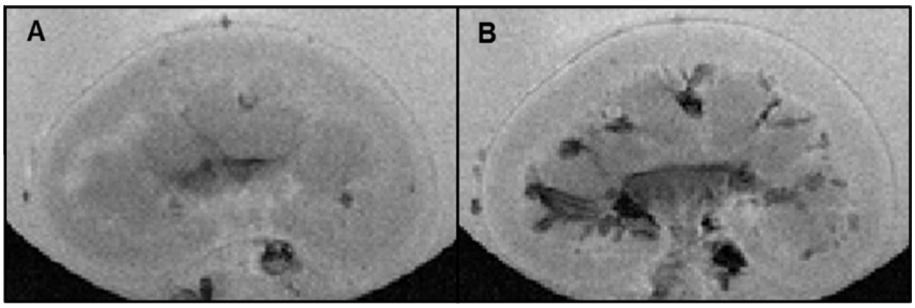

Fig. 8. T_2^*-wt MR images of a sheep kidney before (A) and after (B) the administration of TSL-Ho-microgels. The black spots indicate the presence of TSL-Ho-microgels.

on the MR image. After injection of the TSL-Ho-microgels, black spots appeared in the interlobular blood vessels at the start of the cortex of the kidney indicating the presence of clusters of TSL-Ho-microgels. This shows that TSL-Ho-microgels can be visualized by MRI in tissue as expected.

In our work, alginate microgels containing temperature sensitive liposomes were exploited for embolization. Several strategies for embolization have been reported previously. Clinically, a chemotherapeutic drug is administered followed by an embolic particle. This embolic particle reduces the wash out of the drug but still a part of the dose ends up in the blood circulation [22,23]. Drug eluting beads (DEB) were developed to simplify the embolization procedure and to reduce the systemic exposure. These DEBs show a sustained release of the loaded drug [23,24]. On the contrary, our TSL-Ho-microgels show complete and very rapid release after a mild hyperthermia pulse. With this strategy, a higher peak concentration of the drug can be reached in the tumor compared to DEBs. Another advantage is that TSL-Ho-microgels can be visualized by MRI during all stadia of the treatment. Importantly, also the drug release from our TSL-Ho-microgels can be monitored after mild hyperthermia using the MRI agent [Gd(HPDO3A)(H_2O)], which is also present in the aqueous core of the liposomes, as tracer.

4. Conclusion

This paper shows that temperature sensitive MR-imageable microgels that rapidly release their payload upon hyperthermia (42 °C) were successfully developed. The holmium ion content in the microgels was optimized to allow visualization of the microgels by MRI. The temperature triggered release of [Gd(HPDO3A)(H_2O)] was demonstrated with MRI, while fluorescein (a drug mimicking dye) release was visualized with fluorescence microscopy. Fluorescein and [Gd(HPDO3A)(H_2O)] were released at the same rate and extent, indicating that the release of [Gd(HPDO3A)(H_2O)] is expected to be a good indicator for the *in vivo* release of a cytostatic drug encapsulated in the aqueous core of the liposomes. It is concluded that these triggerable microgels are attractive systems for real-time, MR-guided embolization and triggered release of drugs.

Acknowledgements

Ullrich Jahnz from GeniaLab® is kindly acknowledged for his advice concerning the JetCutter system and Frederike Huissoon, FMC Biopolymers and IMCD Benelux B.V. for supplying the Manucol LKX. This research was performed within the framework of CTMM, the Center for Translational Molecular Medicine (www.ctmm.nl), Project HIFU-CHEM (Grant 030-301).

References

[1] Maeda H. Tumor-selective delivery of macromolecular drugs via the EPR effect: background and future prospects. Bioconjug Chem 2010;21(5):797–802.
[2] Bae YH, Park K. Targeted drug delivery to tumors: myths, reality and possibility. J Control Release 2011;153(3):198–205.
[3] Lammers T, Kiessling F, Hennink WE, Storm G. Drug targeting to tumors: principles, pitfalls and (pre-) clinical progress. J Control Release 2012;161:175–87.
[4] Duncan R. Polymer therapeutics: top 10 selling pharmaceuticals – what next? J Control Release 2014;190:371–80.
[5] Wang Y, Grainger D. Barriers to advancing nanotechnology to better improve and translate nanomedicines. Front Chem Sci Eng 2014;8:265–75.
[6] Torchilin VP. Targeted pharmaceutical nanocarriers for cancer therapy and imaging. AAPS J 2007;9:E128–47.
[7] Torchilin VP. Recent advances with liposomes as pharmaceutical carriers. Nat Rev Drug Discov 2005;4:145–60.
[8] Svenson S. Clinical translation of nanomedicines. Curr Opin Solid State Mater Sci 2012;16:287–94.
[9] Barenholz Y. Doxil (R) – the first FDA-approved nano-drug: lessons learned. J Control Release 2012;160(2):117–34.
[10] Allen TM, Cullis PR. Liposomal drug delivery systems: from concept to clinical applications. Adv Drug Deliv Rev 2013;65(1):36–48.
[11] Northfelt DW, Dezube BJ, Thommes JA, Miller BJ, Fischl MA, Friedman-Kien A, et al. Pegylated-liposomal doxorubicin versus doxorubicin, bleomycin, and vincristine in the treatment of AIDS-related Kaposi's sarcoma: results of a randomized phase III clinical trial. J Clin Oncol 1998;16(7):2445–51.
[12] O'Brien ME, Wigler N, Inbar M, Rosso R, Grischke E, Santoro A, et al. Reduced cardiotoxicity and comparable efficacy in a phase III trial of pegylated liposomal doxorubicin HCl (CAELYX/Doxil) versus conventional doxorubicin for first-line treatment of metastatic breast cancer. Ann Oncol 2004;15:440–9.
[13] Harris L, Batist G, Belt R, Rovira D, Navari R, Azarnia N, et al. Liposome-encapsulated doxorubicin compared with conventional doxorubicin in a randomized multicenter trial as first-line therapy of metastatic breast carcinoma. Cancer 2002;94:25–36.
[14] Jain RK, Stylianopoulos T. Delivering nanomedicine to solid tumors. Nat Rev Clin Oncol 2010;7(11):653–64.
[15] Needham D, Anyarambhatla G, Kong G, Dewhirst MW. A new temperature-sensitive liposome for use with mild hyperthermia: characterization and testing in a human tumor xenograft model. Cancer Res 2000;60:1197–201.

[16] van Elk M, Deckers R, Oerlemans C, Shi Y, Storm G, Vermonden T, et al. Triggered release of doxorubicin from temperature-sensitive poly(N-(2-hydroxypropyl)-methacrylamide mono/dilactate) grafted liposomes. Biomacromolecules 2014;15(3):1002–9.
[17] Tagami T, May JP, Ernsting MJ, Li S. A thermosensitive liposome prepared with a Cu^{2+} gradient demonstrates improved pharmacokinetics, drug delivery and antitumor efficacy. J Control Release 2012;161(1):142–9.
[18] Limmer S, Hahn J, Schmidt R, Wachholz K, Zengerle A, Lechner K, et al. Gemcitabine treatment of rat soft tissue sarcoma with phosphatidyldiglycerol-based thermosensitive liposomes. Pharm Res 2014;31(9):2276–86.
[19] Kong G, Anyarambhatla G, Petros WP, Braun RD, Colvin OM, Needham D, et al. Efficacy of liposomes and hyperthermia in a human tumor xenograft model: importance of triggered drug release. Cancer Res 2000;60(24):6950–7.
[20] Manzoor AA, Lindner LH, Landon CD, Park J, Simnick AJ, Dreher MR, et al. Overcoming limitations in nanoparticle drug delivery: triggered, intravascular release to improve drug penetration into tumors. Cancer Res 2012;72(21):5566–75.
[21] Li L, ten Hagen TLM, Haeri A, Soullie T, Scholten C, Seynhaeve ALB, et al. A novel two-step mild hyperthermia for advanced liposomal chemotherapy. J Control Release 2014;174:202–8.
[22] Brown DB, Gould JE, Gervais DA, Goldberg SN, Murthy R, Millward SF, et al. Transcatheter therapy for hepatic malignancy: standardization of terminology and reporting criteria. J Vasc Interv Radiol 2009;20(7 Suppl):S425–34.
[23] Lewandowski RJ, Geschwind J, Liapi E, Salem R. Transcatheter intraarterial therapies: rationale and overview. Radiology 2011;259(3):641–57.
[24] Lencioni R. Loco-regional treatment of hepatocellular carcinoma in the era of molecular targeted therapies. Oncology 2010;78:107–12.
[25] Hong K, Khwaja A, Liapi E, Torbenson MS, Georgiades CS, Geschwind JFH. New intra-arterial drug delivery system for the treatment of liver cancer: preclinical assessment in a rabbit model of liver cancer. Clin Cancer Res 2006;12(8):2563–7.
[26] Lewis AL, Dreher MR. Locoregional drug delivery using image-guided intra-arterial drug eluting bead therapy. J Control Release 2012;161(2):338–50.
[27] Chung E, Kim H, Lee G, Kwak B, Jung J, Kuh H, et al. Design of deformable chitosan microspheres loaded with superparamagnetic iron oxide nanoparticles for embolotherapy detectable by magnetic resonance imaging. Carbohydr Polym 2012;90(4):1725–31.
[28] Kim JS, Kwak BK, Shim HJ, Lee YC, Baik HW, Lee MJ, et al. Preparation of doxorubicin-containing chitosan microspheres for transcatheter arterial chemoembolization of hepatocellular carcinoma. J Microencapsul 2007;24(5):408–19.
[29] Chen J, Sheu AY, Li W, Zhang Z, Kim D, Lewandowski RJ, et al. Poly(lactide-co-glycolide) microspheres for MRI-monitored transcatheter delivery of sorafenib to liver tumors. J Control Release 2014;184:10–7.
[30] Forster REJ, Thuermer F, Wallrapp C, Lloyd AW, Macfarlane W, Phillips GJ, et al. Characterisation of physico-mechanical properties and degradation potential of calcium alginate beads for use in embolisation. J Mater Sci – Mater Med 2010;21(7):2243–51.
[31] Lewis AL, Gonzalez MV, Lloyd AW, Hall B, Tang YQ, Willis SL, et al. DC bead: in vitro characterization of a drug-delivery device for transarterial chemoembolization. J Vasc Interv Radiol 2006;17(2):335–42.
[32] Lewis AL, Holden RR. DC bead embolic drug-eluting bead: clinical application in the locoregional treatment of tumours. Expert Opin Drug Deliv 2011;8(2):153–69.
[33] Poon RT, Tso WK, Pang RW, Ng KK, Woo R, Tai KS, et al. A phase I/II trial of chemoembolization for hepatocellular carcinoma using a novel intra-arterial drug-eluting bead. Clin Gastroenterol Hepatol 2007;5(9):1100–8.
[34] Varela M, Real MI, Burrel M, Forner A, Sala M, Brunet M, et al. Chemoembolization of hepatocellular carcinoma with drug eluting beads: efficacy and doxorubicin pharmacokinetics. J Hepatol 2007;46(3):474–81.
[35] Dhanasekaran R, Kooby DA, Staley CA, Kauh JS, Khanna V, Kim HS. Comparison of conventional transarterial chemoembolization (TACE) and chemoembolization with doxorubicin drug eluting beads (DEB) for unresectable hepatocelluar carcinoma (HCC). J Surg Oncol 2010;101(6):476–80.
[36] Nicolini D, Svegliati-Baroni G, Candelari R, Mincarelli C, Mandolesi A, Bearzi I, et al. Doxorubicin-eluting bead vs conventional transcatheter arterial chemoembolization for hepatocellular carcinoma before liver transplantation. World J Gastroenterol 2013;19(34):5622–32.
[37] Gasselhuber A, Dreher MR, Rattay F, Wood BJ, Haemmerich D. Comparison of conventional chemotherapy, stealth liposomes and temperature-sensitive liposomes in a mathematical model. PLoS ONE 2012;7(10).
[38] Kerr DJ, Kerr AM, Freshney RI, Kaye SB. Comparative intracellular uptake of adriamycin and 4′-deoxydoxorubicin by nonsmall cell lung tumor cells in culture and its relationship to cell survival. Biochem Pharmacol 1986;35(16):2817–23.
[39] Oerlemans C, Seevinck PR, Smits ML, Hennink WE, Bakker CJG, van den Bosch MAAJ, et al. Holmium–lipiodol–alginate microspheres for fluoroscopy-guided embolotherapy and multimodality imaging. Int J Pharm 2015;482(1–2):47–52.
[40] Lencioni R, de Baere T, Burrel M, Caridi JG, Lammer J, Malagari K, et al. Transcatheter treatment of hepatocellular carcinoma with doxorubicin-loaded DC Bead (DEBDOX): technical recommendations. Cardiovasc Intervent Radiol 2012;35(5):980–5.
[41] Ko JA, Lee YL, Jeong HJ, Park HJ. Preparation of encapsulated alliinase in alginate microparticles. Biotechnol Lett 2012;34(3):515–8.
[42] Park H, Kim P, Hwang T, Kwon O, Park T, Choi S, et al. Fabrication of cross-linked alginate beads using electrospraying for adenovirus delivery. Int J Pharm 2012;427(2):417–25.
[43] Hanus J, Ullrich M, Dohnal J, Singh M, Stepanek F. Remotely controlled diffusion from magnetic liposome microgels. Langmuir 2013;29(13):4381–7.
[44] Prusse U, Dalluhn J, Breford J, Vorlop KD. Production of spherical beads by JetCutting. Chem Eng Technol 2000;23(12):1105–10.
[45] Oerlemans C, Seevinck PR, van de Maat GH, Boulkhrif H, Bakker CJG, Hennink WE, et al. Alginate–lanthanide microspheres for MRI-guided embolotherapy. Acta Biomater 2013;9(1):4681–7.
[46] Dai CY, Wang BC, Zhao HW, Li B, Wang H. Preparation and characterization of liposomes-in-alginate (LIA) for protein delivery system. Colloids Surf, B 2006;47(2):205–10.
[47] Cohen R, Kanaan H, Grant GJ, Barenholz Y. Prolonged analgesia from Bupisome and Bupigel formulations: from design and fabrication to improved stability. J Control Release 2012;160(2):346–52.
[48] Ullrich M, Hanus J, Dohnal J, Stepanek F. Encapsulation stability and temperature-dependent release kinetics from hydrogel-immobilised liposomes. J Colloid Interface Sci 2013;394:380–5.
[49] Zielhuis SW, Seppenwoolde JH, Bakker CJG, Jahnz U, Zonnenberg BA, van het Schip AD, et al. Characterization of holmium loaded alginate microspheres for multimodality imaging and therapeutic applications. J Biomed Mater Res A 2007;82A(4):892–8.
[50] Li S, Wang X, Zhang X, Yang R, Zhang H, Zhu L, et al. Studies on alginate–chitosan microcapsules and renal arterial embolization in rabbits. J Control Release 2002;84(3):87–98.
[51] Eroglu M, Kursaklioglu H, Misirli Y, Iyisoy A, Acar A, Dogan AI, et al. Chitosan-coated alginate microspheres for embolization and/or chemoembolization: in vivo studies. J Microencapsul 2006;23(4):367–76.
[52] Negussie AH, Yarmolenko PS, Partanen A, Ranjan A, Jacobs G, Woods D, et al. Formulation and characterisation of magnetic resonance imageable thermally sensitive liposomes for use with magnetic resonance-guided high intensity focused ultrasound. Int J Hyperthermia 2011;27(2):140–55.
[53] Ponce AM, Viglianti BL, Yu D, Yarmolenko PS, Michelich CR, Woo J, et al. Magnetic resonance imaging of temperature-sensitive liposome release: drug dose painting and antitumor effects. J Natl Cancer Inst 2007;99(1):53–63.
[54] Anyarambhatla GR, Needham D. Enhancement of the phase transition permeability of DPPC liposomes by incorporation of MPPC: a new temperature-sensitive liposome for use with mild hyperthermia. J Liposome Res 1999;9:491–506.
[55] Li L, ten Hagen TLM, Schipper D, Wijnberg TM, van Rhoon GC, Eggermont AMM, et al. Triggered content release from optimized stealth thermosensitive liposomes using mild hyperthermia. J Control Release 2010;143(2):274–9.
[56] Lindner LH, Eichhorn ME, Eibl H, Teichert N, Schmitt-Sody M, Issels RD, et al. Novel temperature-sensitive liposomes with prolonged circulation time. Clin Cancer Res 2004;10(6):2168–78.
[57] DeRamos CM, Irwin AE, Nauss JL, Stout BE. C-13 NMR and molecular modeling studies of alginic acid binding with alkaline earth and lanthanide metal ions. Inorg Chim Acta 1997;256(1):69–75.
[58] Smits ML, Nijsen JF, van den Bosch MA, Lam MG, Vente MA, Mali WP, et al. Holmium-166 radioembolisation in patients with unresectable, chemorefractory liver metastases (HEPAR trial): a phase 1, dose-escalation study. Lancet Oncol 2012;13(10):1025–34.

[59] Bruce DW, Hietbrink BE, DuBois KP. The acute mammalian toxicity of rare earth nitrates and oxides. Toxicol Appl Pharmacol 1963;5(6):750–9.
[60] Haley TJ, Koste L, Komesu N, Efros M, Upham HC. Pharmacology and toxicology of dysprosium, holmium, and erbium chlorides. Toxicol Appl Pharmacol 1966;8(1):37–43.
[61] http://www.microscopyu.com/tutorials/java/phasecontrast/shadeoff/ [accessed December 2014].
[62] Decho AW. Imaging an alginate polymer gel matrix using atomic force microscopy. Carbohydr Res 1999;315(3–4):330–3.
[63] Turco G, Donati I, Grassi M, Marchioli G, Lapasin R, Paoletti S. Mechanical spectroscopy and relaxometry on alginate hydrogels: a comparative analysis for structural characterization and network mesh size determination. Biomacromolecules 2011;12(4):1272–82.
[64] Cvetkovic A, Picioreanu C, Straathof A, Krishna R, van der Wielent L. Relation between pore sizes of protein crystals and anisotropic solute diffusivities. J Am Chem Soc 2005;127(3):875–9.